Matter and Radiation at Extremes | RESEARCH ARTICLE | scitation.org/journal/mre

A novel square planar N_4^{2-} ring with aromaticity in BeN_4

Cite as: Matter Radiat. Extremes 7, 038401 (2022); doi: 10.1063/5.0084802
Submitted: 10 January 2022 • Accepted: 13 March 2022 •
Published Online: 4 April 2022

Jiani Lin,[1,2] Fangxu Wang,[3] Qi Rui,[3] Jianfu Li,[1,a)] Qinglin Wang,[4] and Xiaoli Wang[1,a)]

AFFILIATIONS

[1]School of Physics and Electronic Information, Yantai University, Yantai 264005, People's Republic of China
[2]Beijing Computational Science Research Center, Beijing 100193, People's Republic of China
[3]School of Physics and Electronic Engineering, Linyi University, Linyi 276005, People's Republic of China
[4]Shandong Key Laboratory of Optical Communication Science and Technology, School of Physical Science and Information Technology, Liaocheng University, Liaocheng 252059, People's Republic of China

[a)]**Authors to whom correspondence should be addressed:** jianfuli@ytu.edu.cn and xlwang@ytu.edu.cn

ABSTRACT

A structural search leads to the prediction of a novel alkaline earth nitride BeN_4 containing a square planar N_4^{2-} ring. This compound has a particular chemical bonding pattern giving it potential as a high-energy-density material. The *P*4/*nmm* phase of BeN_4 may be stable under ambient conditions, with a bandgap of 3.72 eV. It is predicted to have high thermodynamic and kinetic stability due to transfer of the outer-shell *s* electrons of the Be atom to the N_4 cluster, with the outer-shell 2*p* orbital accommodating the lone-pair electrons of N_4^{2-}. The total of six π electrons is the most striking feature, indicating that the square planar N_4^{2-} exhibits aromaticity. Under ambient conditions, BeN_4 has a high energy density (3.924 kJ/g relative to Be_3N_2 and N_2 gas), and its synthesis might be possible at pressures above 31.6 GPa.

I. INTRODUCTION

Polymeric nitrogen containing single and double nitrogen bonds releases a large amount of energy during its decomposition and is thus a candidate green high-energy-density material (HEDM). However, the synthesis of stable HEDMs containing breakable single or double nitrogen bonds poses a real challenge. To date, there has been experimental confirmation of four polymeric nitrogen structures: cg-N (synthesized at 2000 K and 110 GPa),[1] LP-N (3000 K and 150 GPa),[2] HLP-N (3300 K and 244 GPa),[3] and bp-N (2200 K and 146 GPa).[4] However, these structures are synthesized under high temperatures and pressures, which limits their application as HEDMs. Therefore, it is an urgent, although formidable, challenge to explore novel polymeric nitrogen structures that can be synthesized under mild conditions.

Numerous theoretical and experimental results have indicated that the addition of metallic elements (M) to the nitrogen materials could provide new compound forms of polymeric nitrogen (MN_x) at lower pressures. Compared with pure polymeric nitrogen structures, these may have higher stability and milder synthesis conditions. Charge transfer from metal to polynitrogen may play important roles in reducing the pressure required for synthesis and improving structural stability. Theoretical calculations have predicted a variety of polynitride compounds MN_x (M = Li, Be, Na, Mg, Al, K, Ca, Cs, Rb, Ba, Se, He, or Xe, with x = 3, 5, 6, 10) featuring a variety of N_5 or N_6 polymeric nitrogen chains[5–30] and some complicated nitrogen clusters [fused N_{18} rings in KN_8 (Ref. 8) and N_{10} rings in BeN_4 (Ref. 29), etc.]. The transition metals (Sc,[31,32] Mo,[33] Tc,[34] Re,[35] Fe,[36,37] Ru,[38] Os,[39] Rh,[40] Ir,[39] Pd,[41] Pt,[41] Cu,[42] Ag,[43] Au,[44] Zn,[45] and Hg[46]) can also form nitrogen-containing structures. Some of these compounds are not potential HEDMs, but they do prove that introducing metallic elements to nitrogen seems to be a feasible way to enhance metastability. Experimentally, some metals or their compounds have been used as raw materials to synthesize polynitrogen compounds at relatively low pressures. CsN_5 has been successfully synthesized by compressing CsN_3 with N_2 near 60 GPa,[47] and solid LiN_5 solid has been obtained by compression and laser heating of Li embedded in molecular N_2 at 45 GPa.[48] Fe_3N_2, FeN_2, and FeN_4 have been synthesized from Fe and N_2 under different pressures,[49] and elemental Cu reacts with N_2 to form CuN_2 at 50 GPa.[50] Very recently, a beryllium tetranitride *tr*-BeN_4 in the triclinic phase has been synthesized at 85 GPa,[51] and it has similar structural units as the previously predicted *P*-1 BeN_4 (infinite N chains coordinating Be atoms),

proving that crystal structure prediction (CSP) searches can provide credible results.

The alkaline earth metals Be, Mg, Ca, Sr, and Ba are adjacent to the alkali metals in the Periodic Table, with similar properties but with a wider scope for chemical reactions and compound formation because of their additional valence electron. Among the alkaline earths, Be has the lowest atomic weight, and therefore its compounds with nitrogen have a high mass density of N and are good candidate HEDMs. A layered material, BeN_4, containing corrugated N_{10} rings has recently been synthesized.[51] Such a single-bonded polymeric nitrogen network has been predicted theoretically.[29,52] Therefore, we have used an unbiased structural search with a particle-swarm optimization (PSO) algorithm[53,54] to predict new beryllium nitrides with 1:4 compositions and have thereby found a new BeN_4 compound that may be stable at ambient pressure. In this compound, a planar N_4^{2-} ring is surrounded by four Be atoms, and the six π electrons of this ring conform to the Hückel $[4n + 2]$ rule (with $n = 1$), indicating aromaticity of BeN_4. The large mass ratio of nitrogen in this compound (86.15%) leads to a high energy density (3.924 kJ/g).

II. COMPUTATIONAL DETAILS

We used the Crystal Structure Analysis by Particle Swarm Optimization (CALYPSO) code[53,54] to search the structures of BeN_4 at different pressures, namely, 0, 10, 20, 50, and 100 GPa, at 0 K. Geometrical optimizations, total energy calculations, and electronic structure calculations were carried out in the framework of density functional theory (DFT) using the generalized gradient approximation with the Perdew–Burke–Ernzerhof functional (GGA-PBE),[55] with a cutoff energy of 500 eV and a 0.03 $Å^{-1}$ k-point grid[56] in the Vienna *Ab initio* Simulation Package (VASP).[57] The convergence threshold was used to optimize the atomic positions and lattice constants until the forces on each atom were less than 0.01 eV/Å and the energy change was less than 1.0×10^{-6} eV/atom. Projector augmented wave (PAW)[58] pseudopotentials were adopted for Be and N, with $1s^2 2s^2$ and $2s^2 2p^3$ valence states, respectively. Phonon dispersion relations were calculated using a supercell method with the finite displacement approach[59] through the Phonopy code.[60] *Ab initio* molecular dynamics (AIMD) simulations were performed within the NVE ensemble[61,62] to study thermal stability. The strain–stress methodology was used to calculate the elastic constants. The bulk and shear modulus, Young's modulus E, and Poisson's ratio ν were obtained from the Voigt–Reuss–Hill approximations.[63] The detonation velocity and pressure were calculated through the Kamlet–Jacobs semiempirical equations $V_d = 1.01(NM^{0.5}E_d^{0.5})^{0.5}(1 + 1.30\rho)$ and $P_d = 15.58\rho^2 NM^{0.5}E_d$,[64,65] where N is the number of moles of gas per gram, M is the molar mass of the N_2 gas (28 g/mol), E_d is the energy density, and ρ is the mass density of BeN_4. The crystal orbital Hamilton population (COHP) was calculated to characterize the bonding properties using the LOBSTER program.[66] Charge transfer was based on a Bader analysis,[56,67] and the chemical bonding mode was calculated by the Solid State Adaptive Natural Density Partitioning (SSAdNDP) method.[68]

III. RESULTS AND DISCUSSION

A. Geometric structures

In a previous study, Zhang *et al.*[29] used an unbiased structure search method to explore the structural evolutionary behaviors of beryllium polynitride compounds below 200 GPa. Interestingly, the only stable N-rich composition was found to be BeN_4, with the compounds $P1$-BeN_4 and $P2_1/c$-BeN_4 being theoretically predicted to exist at high pressure. In our work, also using an unbiased structure search method with CALYPSO, we have predicted a new BeN_4 in the tetragonal phase with the high group symmetry of $P4/nmm$. The calculated enthalpies of these three structures at pressures from 0 to 130 GPa at $T = 0$ K are shown in Fig. 1.

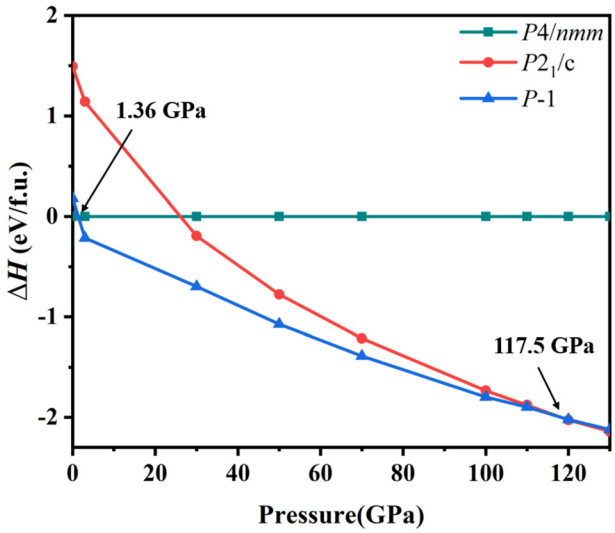

FIG. 1. Enthalpy difference of BeN_4 relative to the $P4/nmm$ structure under high pressure. $P1$-BeN_4 and $P2_1/c$- BeN_4 are previously known high-pressure structures from Ref. 29. The phase transition pressures are indicated by the arrows.

BeN_4 undergoes structural phase transitions first from $P4/nmm$ to $P1$ at a pressure of 1.36 GPa and then to $P2_1/c$ at 117.5 GPa. The phase transition pressure from $P1$ to $P2_1/c$ phase that we calculated is similar to the reported value (115.1 GPa) in Fig. 1, which indicates that our method is appropriate. The predicted crystal structure of $P4/nmm$ and its corresponding lattice parameters and atomic coordinates are shown in Fig. 2 and Table I, respectively. According to Fig. 2, there is a square planar N_4^{2-} ring in $P4/nmm$-BeN_4, where each inner N atom is shared by one Be atom and two adjacent N atoms. Within the *cyclo*-N_4, the

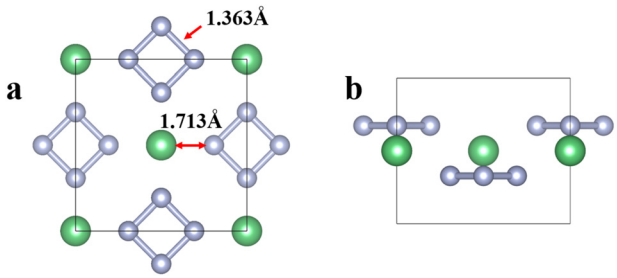

FIG. 2. Crystal structure of the stable $P4/nmm$-BeN_4 at ambient pressure: (a) side view along c axis; (b) a axis. The green spheres are Be atoms and the gray spheres N atoms.

TABLE I. Lattice parameters and atomic positions for *P*4/*nmm*-BeN_4 at 0 GPa.

Space group	Pressure (GPa)	Lattice parameter (Å°)	Atom	Wyckoff position	*x*	*y*	*z*
P4/*nmm*	0	$a = 5.03$ $\alpha = 90.00$	Be	4e	0.500	0.500	0.500
		$b = 5.03$ $\beta = 90.00$	N	16k	0.000	0.692	0.327
		$c = 4.21$ $\gamma = 90.00$					

length of the N–N bond is 1.363 Å and the angles of the N–N–N bonds are all around 90° at ambient pressure. Be atoms are situated at the center or vertex positions, with each Be atom binding to four adjacent N atoms with equal bond lengths of 1.713 Å. A variety of N_4 clusters have been predicted theoretically,[24,30,69–71] including N_4^{4-}, N_4^{2+}, N_4^{2-}, and N_4^{+}. However, the novel square planar N_4^{2-} ring predicted in the present work has not previously been reported, although a square planar N_4^{2-} ring was found in bipyramidal Li_2N_4 by van Zandwijk *et al.*,[72] and a series of alkali metal compounds M_2N_4 and alkaline earth compounds MN_4 with D_{4h} bipyramidal, D_{2h} planar, and C_{2v} planar structures were also found to contain such an N_4^{2-} ring.[70,71,73] Here, we shall now focus on the square planar N_4^{2-} ring in *P*4/*nmm*-BeN_4.

B. Kinetic and thermodynamic stability

Because there are no imaginary frequencies in the entire Brillouin zone (Fig. 3), the calculated phonon dispersions show that *P*4/*nmm*-BeN_4 is dynamically stable at ambient pressure. In addition, the phonon density of states shows that the low-frequency vibrational mode can be mostly attributed to the strong coupling vibration between Be and N atoms, while the N–N stretching mode is responsible for the high-frequency vibrational mode.

We further explore the thermal stability of BeN_4 at ambient pressure and high temperature by performing AIMD simulations on a $3 \times 2 \times 3$ supercell containing 180 atoms. The images of the geometrical structure in Figs. 4(a) and 4(b) clearly reveal that the square planar N_4^{2-} ring maintains its structural integrity without any visible distortion after heating at 300 or 500 K for 10 ps with a time step of 1 fs. The radial distribution function (RDF) of N–N separations in *P*4/*nmm*-BeN_4 is shown in Fig. 4(c). The first sharp RDF peak is the average distance between the selected atom and its nearest surrounding atoms, here corresponding to the N–N bonds of BeN_4. This indicates that the N–N bond lengths remain at 1.369 Å as the temperature rises from zero to 500 K, which proves the stability of *P*4/*nmm*-BeN_4 at high temperatures. Thus, BeN_4 has a moderate cohesive energy and good thermal stability.

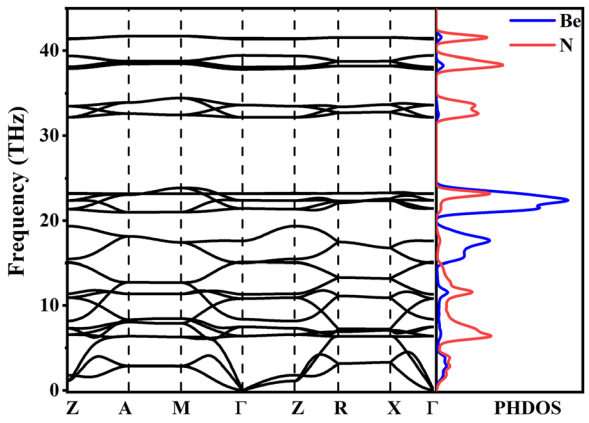

FIG. 3. Phonon dispersions and phonon density of states (PHDOS) of *P*4/*nmm*-BeN_4 at ambient pressure.

C. Mechanical stability

We also calculated the elastic constants of the *P*4/*nmm*-BeN_4 structure because these are helpful for determining the mechanical stability and hardness of a material. The elastic constants C_{ij}, bulk modulus *B*, shear modulus *G*, the Young's modulus *E* and Poisson's ratio *v* of *P*4/*nmm*-BeN_4 are presented in Table II. They are related by $E = 9BG/(3B + G)$ and $v = (3B - 2G)/[2(3B + G)]$.[74] We calculated the bulk modulus of the β-Be_3N_2 hexagonal structure at ambient pressure to be $B = 237.18$ GPa, which is similar to a previously published value for this compound (236 GPa),[75] which indicates that the calculation method we have adopted is appropriate for the Be–N system. The Pugh ratio $k = B/G$ is used to estimate ductile or brittle characteristics, with $k < 1.75$ corresponding to brittle behavior and $k \geq 1.75$ to ductile behavior. The value of *k* for the *P*4/*nmm*-BeN_4 structure is 1.02, indicating that this compound is brittle. For a tetragonal structure to be stable, the C_{ij} should satisfy the Born–Huang stability criteria $C_{11} > 0, C_{33} > 0, C_{44} > 0, C_{66} > 0, C_{11} - C_{12} > 0, C_{11} + C_{33} - 2C_{13} > 0$, and $2(C_{11} + C_{12}) + C_{33} + 4C_{13} > 0$. The elastic constants of *P*4/*nmm*-BeN_4 satisfy these criteria, indicating that it should be mechanically stable under ambient conditions.

D. Explosive performance

Energy density E_d is important for energy storage capability, while detonation velocity V_d and pressure P_d are known to be significant indices of detonation performance. The dissociation energy of *P*4/*nmm*-BeN_4 is calculated for the following decomposition path under ambient conditions: $3BeN_4(s) \rightarrow Be_3N_2(s) + 5N_2(g)$. We use E_d = (96.4853 × BeN_4 molecule energy released)/(molar mass of BeN_4) to calculate the energy density of *P*4/*nmm*-BeN_4, the calculated E_d is about 3.92 kJ/g with reference to the lowest-energy phase at ambient pressure[29,76] (the phase transition in Fig. S1 in the supplementary material). Table III compares the detonation properties of *P*4/*nmm*-BeN_4 with the experimental values for TNT and HMX. Although *P*4/*nmm*-BeN_4 shows superiority only with regard to

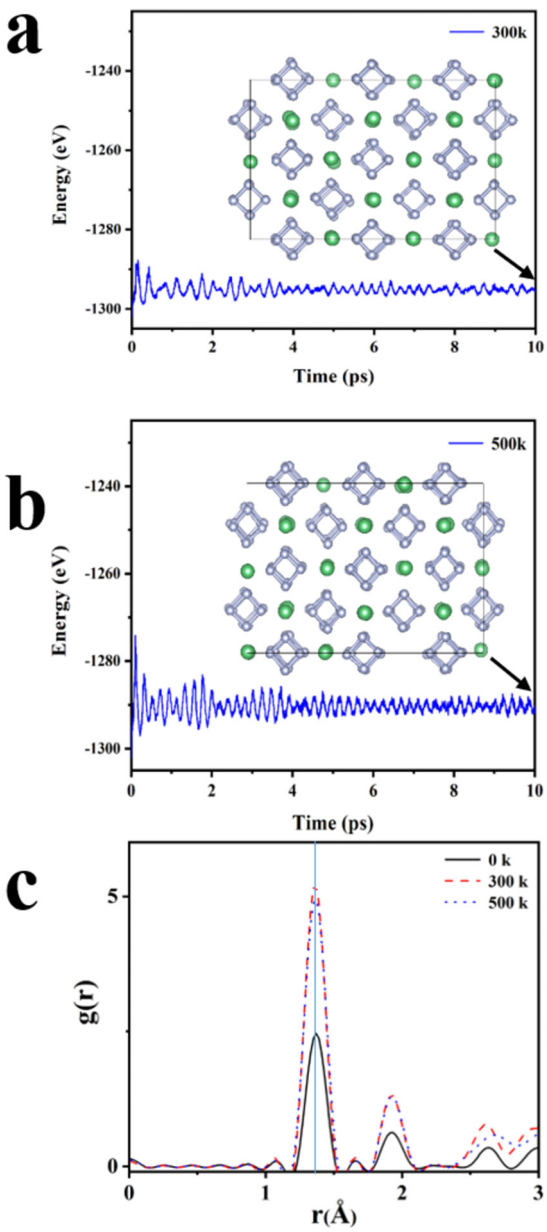

FIG. 4. Molecular dynamics simulations and radial distribution function of *P4/nmm*-BeN_4. (a) and (b) Equilibrium structures at 10 ps and fluctuations of the total potential energies during the AIMD simulation at temperatures of 300 and 500 K, respectively. (c) RDF for N–N separations.

its detonation velocity being higher than that of TNT, its detonation performance does indicate that it has potential application as an explosive.

E. Electronic properties

To illustrate the electronic properties of BeN_4, its band structure, projected density of states (PDOS), and crystal orbital Hamilton populations (COHPs) under ambient conditions are presented in Fig. 5. There are no bands crossing the Fermi level in the band structure in Fig. 5(a), which indicates that the predicted BeN_4 crystal is a semiconductor with a bandgap of 3.67 eV. The obvious overlap between Be 2*p* and N 2*p* in the PDOS [Fig. 5(b)] reveals that the orbitals are strongly hybridized.

TABLE II. Elastic constants of *P4/nmm*-BeN_4 and Be_3N_2 at ambient pressure.

		P4/nmm	Be_3N_2
Elastic stiffness constants C_{ij}	C_{11}	224.82	517.77
	C_{22}		
	C_{33}	20.82	479.98
	C_{44}	111.15	190.16
	C_{55}	2.29	
	C_{66}	2.29	185.58
	C_{12}	6.21	137.45
	C_{13}	20.32	87.57
B (GPa)		41.75	237.18
G (GPa)		41.06	192.14
E (GPa)		92.78	453.87
v		0.13	0.18
k		1.02	

TABLE III. Detonation properties of *P4/nmm*-BeN_4, TNT, and HMX.

Compound	ρ (g/cm^3)	E_d (kJ/g)	V_d (km/s)	P_d (kbar)
P4/nmm-BeN_4	1.01	3.92	7.35	158.11
TNT	1.64[a]	4.30[b]	6.90[c]	190.00[a]
HMX	1.90[a]	5.70[b]	9.10[c]	393.00[a]

[a]Reference 77.
[b]Reference 78.
[c]Reference 79.

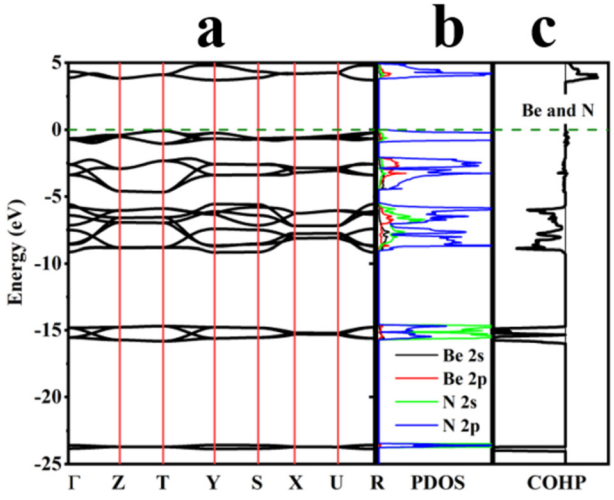

FIG. 5. Electronic properties of *P4/nmm*-BeN_4 at ambient pressure. (a) Band structure. (b) PDOS of Be and N atoms. (c) COHP between N and N atoms.

Therefore, the bonding between Be and N is partially covalent. To characterize the orbital interaction between two N atoms, we performed a COHP analysis to measure the overlap strength between two N atoms. Negative values correspond to bonding states and positive values to antibonding states in Fig. 5(c), where it can be seen that the bonding states between N and N in BeN_4 are completely occupied and the antibonding states partially occupied, resulting in strong covalent bonding. The integrated COHPs (ICOHPs) calculated from the wave function's energy-weighted population between two atomic orbitals represent the bonding strength. The ICOHP values of N–N and Be–N bonds are −12.21 and −1.63 eV, respectively. Therefore, the N–N interaction is substantially stronger than the Be–N interaction, which indicates that the covalent bonding between Be and N is weaker, which is consistent with the results of our previous hybridization investigation. Moreover, the Bader charges of Be and N atoms shown in Table S1 in the supplementary material reveal that the Be atoms combine with the N atoms primarily through electrostatic forces. Thus, the Be–N bonding has both covalent and ionic character.

F. Chemical bonding pattern

We analyzed the chemical bonding patterns in the *P*4/*nmm*-BeN_4 crystal using SSAdNDP software. In a primitive cell, Be atoms connect four neighboring N_4 rings via four two-center, two-electron (2c-2e) Be–N σ bonds [Fig. 6(a)], and four N atoms form a ring through four 2c-2e N–N σ bonds [Fig. 6(b)]. There are two types of π orbital [Figs. 6(c) and 6(d)]: one links two adjacent N atoms through two 2c-2e N–N π bonds, while the other links four N atoms via one four-center, two-electron (4c-2e) N–N large π bond in a plane. Together, the σ and π bonds require $2 \times 11 = 22$ electrons, which is equal to the number of outer valence electrons of BeN_4. It can be seen that the localized 2c-2e σ bonds, 2c-2e π bonds, and delocalized 4c-2e π bonds have an influence on the high structural stability of BeN_4. The total of six π electrons is the most striking feature, since it satisfies the Hückel $[4n + 2]$ rule (with $n = 1$), indicating that BeN_4 is an aromatic structure.

The band structure, PDOS, COHP calculations, and chemical bonding pattern analysis illustrate the covalent bonding between the N atoms. The Be atoms contribute their outer-shell electrons to the N_4 cluster and use the outer-shell 2*p* orbital to accommodate the lone-pair electrons of N_4^{2-}, with the formation of covalent and ionic bonds to stabilize the crystal. This explains why Be can stabilize the square N_4 ring.

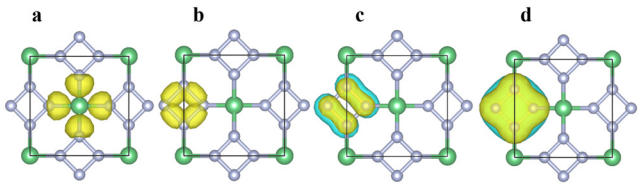

FIG. 6. SSAdNDP-derived chemical bonding pattern of *P*4/*nmm*-BeN_4 at ambient pressure: (a) $4 \times$ 2c-2e Be–N σ bonds, ON = 1.65|e|, iso-value = 0.15; (b) $4 \times$ 2c-2e N–N σ bonds, ON = 1.65|e|, iso-value = 0.2; (c) $2 \times$ 2c-2e N–N π bonds, ON = 1.65|e|, iso-value = 0.1; (d) $1 \times$ 4c-2e N–N large π bond, ON = 1.70|e|, iso-value = 0.03.

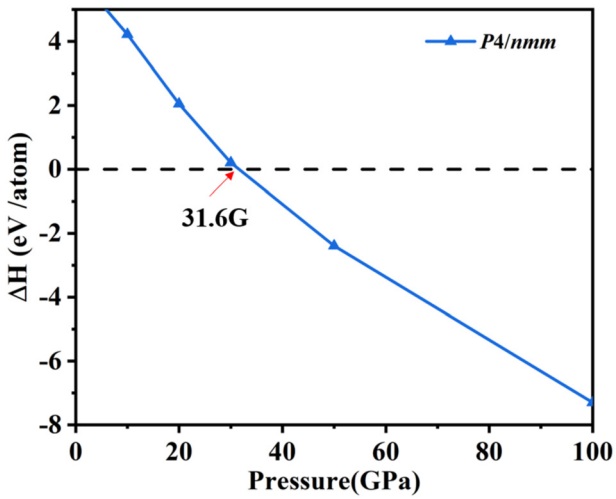

FIG. 7. Enthalpy of formation of *P*4/*nmm*-BeN_4 relative to Be_3N_2 and N_2.

G. Synthetic route to square planar N_4^{2-} ring

Be_3N_2 with two known phases (α[80,81] and β[82]) has been experimentally synthesized. We have calculated the enthalpy of formation of the predicted *P*4/*nmm*-BeN_4 relative to Be_3N_2 and N_2 (the phase transition in Fig. S1 in the supplementary material) to find a possible high-pressure synthetic path. Based on the results in Fig. 7, the predicted BeN_4 can be synthesized through mixing Be_3N_2 and N_2 together at pressures above 31.6 GPa, which indicates that square planar N_4^{2-} can be synthesized beyond 31.6 GPa. It should be noted that both the $P2_1/c$ and *P*-1 phases have lower energies than the *P*4/*nmm* phase above 31.6 GPa (Fig. 1), which makes the synthesis of *P*4/*nmm*-BeN_4 a difficult task. Fortunately, a number of experimental results achieved with high-pressure techniques can provide inspiration for the synthesis of *P*4/*nmm*-BeN_4. The recently synthesized bp-N is not the phase with the lowest energy at the corresponding pressure.[4,83] Similarly, silicon and ice can form different phases along different pressure–temperature paths.[84,85] We anticipate that experimental investigations will also find the precise pressure and temperature conditions for the synthesis of *P*4/*nmm*-BeN_4.

IV. CONCLUSIONS

Through structural searches and density functional calculations under ambient conditions, we have found a *P*4/*nmm*-BeN_4 structure with high kinetic and thermodynamic stability. The phonon dispersion and electronic properties of this structure indicate the presence of covalent bonding between two N atoms, with covalent and ionic bonding between Be^{2+} and square planar N_4^{2-} enhancing the stability of the semiconductor BeN_4 structure. The total of six π electrons satisfies the Hückel $[4n + 2]$ rule (with $n = 1$), indicating that BeN_4 has an aromatic structure. Furthermore, the energy density of *P*4/*nmm*-BeN_4 is 3.92 kJ/g, making it a candidate high-energy-density material. The calculated formation of enthalpy of BeN_4 indicates that the square planar N_4^{2-} ring might be synthesized through mixing Be_3N_2 and N_2 at 31.6 GPa. The results of this investigation of the role of novel chemical bonds in nitrogen chemistry should encourage experimental efforts to synthesize these promising high-energy materials.

SUPPLEMENTARY MATERIAL

See the supplementary material for Figure S1 and Table S1.

ACKNOWLEDGMENTS

This work was supported by the National Natural Science Foundation of China under Grant Nos. 11974154, 11674144, and 11604133, and the Natural Science Foundation of Shandong Province under Grant Nos. ZR2018MA038, 2019GGX103023, Z2018S008, and 2019KJJ019.

AUTHOR DECLARATIONS

Conflict of Interest

The authors have no conflicts to disclose.

DATA AVAILABILITY

All data discussed in the paper are available upon request.

REFERENCES

[1]M. I. Eremets, A. G. Gavriliuk, I. A. Trojan, D. A. Dzivenko, R. Boehler, and R. Academy, "Single-bonded cubic form of nitrogen," Nat. Mater. **3**, 558–563 (2004).
[2]D. Tomasino, M. Kim, J. Smith, and C. S. Yoo, "Pressure-induced symmetry-lowering transition in dense nitrogen to layered polymeric nitrogen (LP-N) with colossal Raman intensity," Phys. Rev. Lett. **113**, 205502 (2014).
[3]D. Laniel, G. Geneste, G. Weck, M. Mezouar, and P. Loubeyre, "Hexagonal layered polymeric nitrogen phase synthesized near 250 GPa," Phys. Rev. Lett. **122**, 066001 (2019).
[4]C. Ji, A. A. Adeleke, L. Yang, B. Wan, H. Gou, Y. Yao, B. Li, Y. Meng, J. S. Smith, V. B. Prakapenka, W. Liu, G. Shen, W. L. Mao, and H. K. Mao, "Nitrogen in black phosphorus structure," Sci. Adv. **6**, eaba9206 (2020).
[5]Q. Wei, C. Zhao, M. Zhang, H. Yan, B. Wei, and X. Peng, "New stable structures of HeN_3 predicted using first-principles calculations," J. Alloys Compd. **800**, 505–511 (2019).
[6]Z. Liu, D. Li, S. Wei, W. Wang, F. Tian, K. Bao, D. Duan, H. Yu, B. Liu, and T. Cui, "Bonding properties of aluminum nitride at high pressure," Inorg. Chem. **56**, 7494–7500 (2017).
[7]Z. Liu, D. Li, S. Wei, Y. Liu, F. Tian, D. Duan, and T. Cui, "Nitrogen-rich GaN_5 and GaN_6 as high energy density materials with modest synthesis condition," Phys. Lett. A **383**, 125859 (2019).
[8]B. A. Steele and I. I. Oleynik, "Novel potassium polynitrides at high pressures," J. Phys. Chem. A **121**, 8955–8961 (2017).
[9]M. Zhang, H. Yan, Q. Wei, and H. Liu, "A new high-pressure polymeric nitrogen phase in potassium azide," RSC Adv. **5**, 11825–11830 (2015).
[10]Y. Shen, A. R. Oganov, G. Qian, J. Zhang, H. Dong, Q. Zhu, and Z. Zhou, "Novel lithium-nitrogen compounds at ambient and high pressures," Sci. Rep. **5**, 14204 (2015).
[11]P. Hou, L. Lian, Y. Cai, B. Liu, B. Wang, S. Wei, and D. Li, "Structural phase transition and bonding properties of high-pressure polymeric CaN_3," RSC Adv. **8**, 4314–4320 (2018).
[12]A. S. Williams, B. A. Steele, and I. I. Oleynik, "Novel rubidium poly-nitrogen materials at high pressure," J. Chem. Phys. **147**, 234701 (2017).
[13]S. Wei, D. Li, Z. Liu, X. Li, F. Tian, D. Duan, B. Liu, and T. Cui, "Alkaline-earth metal (Mg) polynitrides at high pressure as possible high-energy materials," Phys. Chem. Chem. Phys. **19**, 9246–9252 (2017).
[14]L. Zhang, Y. Wang, J. Lv, and Y. Ma, "Materials discovery at high pressures," Nat. Rev. Mater. **2**, 17005 (2017).
[15]W. Wang, H. Wang, Y. Liu, D. Li, F. Tian, D. Duan, H. Yu, and T. Cui, "High-pressure bonding mechanism of selenium nitrides," Inorg. Chem. **58**, 2397–2402 (2019).
[16]F. Peng, Y. Wang, H. Wang, Y. Zhang, and Y. Ma, "Stable xenon nitride at high pressures," Phys. Rev. B **92**, 094104 (2015).
[17]B. Huang and G. Frapper, "Barium–nitrogen phases under pressure: Emergence of structural diversity and nitrogen-rich compounds," Chem. Mater. **30**, 7623–7636 (2018).
[18]J. Lin, Z. Zhu, Q. Jiang, S. Guo, J. Li, H. Zhu, and X. Wang, "Stable zigzag and tripodal all-nitrogen anion N_4^{4-} in BeN_2," AIP Adv. **9**, 055116 (2019).
[19]F. Peng, Y. Yao, H. Liu, and Y. Ma, "Crystalline LiN_5 predicted from first-principles as a possible high-energy material," J. Phys. Chem. Lett. **6**, 2363–2366 (2015).
[20]L. C. Perera, O. Raymond, W. Henderson, P. J. Brothers, and P. G. Plieger, "Advances in beryllium coordination chemistry," Coord. Chem. Rev. **352**, 264–290 (2017).
[21]S. B. Schneider, M. Mangstl, G. M. Friederichs, R. Frankovsky, J. Schmedt auf der Günne, and W. Schnick, "Electronic and ionic conductivity in alkaline earth diazenides $M_{AE}N_2$ (M_{AE} = Ca, Sr, Ba) and in Li_2N_2," Chem. Mater. **25**, 4149–4155 (2013).
[22]S. B. Schneider, R. Frankovsky, and W. Schnick, "Synthesis of alkaline earth diazenides $M_{AE}N_2$ (M_{AE} = Ca, Sr, Ba) by controlled thermal decomposition of azides under high pressure," Inorg. Chem. **51**, 2366–2373 (2012).
[23]S. Yu, B. Huang, Q. Zeng, A. R. Oganov, L. Zhang, and G. Frapper, "Emergence of novel polynitrogen molecule-like species, covalent chains, and layers in magnesium-nitrogen Mg_xN_y phases under high pressure," J. Phys. Chem. C **121**, 11037–11046 (2017).
[24]F. Peng, Y. Han, H. Liu, and Y. Yao, "Exotic stable cesium polynitrides at high pressure," Sci. Rep. **5**, 16902 (2015).
[25]X. Wang, J. Li, N. Xu, H. Zhu, Z. Hu, and L. Chen, "Layered polymeric nitrogen in RbN_3 at high pressures," Sci. Rep. **5**, 16677 (2015).
[26]X. Wang, J. Li, H. Zhu, L. Chen, and H. Lin, "Polymerization of nitrogen in cesium azide under modest pressure," J. Chem. Phys. **141**, 044717 (2014).
[27]X. Wang, J. Li, J. Botana, M. Zhang, H. Zhu, L. Chen, H. Liu, T. Cui, and M. Miao, "Polymerization of nitrogen in lithium azide," J. Chem. Phys. **139**, 164710 (2013).
[28]Y. Li, X. Feng, H. Liu, J. Hao, S. A. T. Redfern, W. Lei, D. Liu, and Y. Ma, "Route to high-energy density polymeric nitrogen *t*-N via He–N compounds," Nat. Commun. **9**, 722 (2018).
[29]S. Zhang, Z. Zhao, L. Liu, and G. Yang, "Pressure-induced stable BeN_4 as a high-energy density material," J. Power Sources **365**, 155–161 (2017).
[30]S. Zhu, F. Peng, H. Liu, A. Majumdar, T. Gao, and Y. Yao, "Stable calcium nitrides at ambient and high pressures," Inorg. Chem. **55**, 7550–7555 (2016).
[31]J. Lin, D. Peng, Q. Wang, J. Li, H. Zhu, and X. Wang, "Stable nitrogen-rich scandium nitrides and their bonding features under ambient conditions," Phys. Chem. Chem. Phys. **23**, 6863–6870 (2021).
[32]M. A. Aslam and Z. J. Ding, "Prediction of thermodynamically stable compounds of the Sc–N system under high pressure," ACS Omega **3**, 11477–11485 (2018).
[33]L.-P. Ding, P. Shao, F.-H. Zhang, C. Lu, and X.-F. Huang, "Prediction of molybdenum nitride from first-principle calculations: Crystal structures, electronic properties, and hardness," J. Phys. Chem. C **122**, 21039–21046 (2018).
[34]Y.-R. Zhao, G.-T. Zhang, H.-Y. Yan, T.-T. Bai, B.-B. Zheng, and Y.-Q. Yuan, "First-principles investigations of the structure and physical properties for new TcN crystal structure," Mol. Phys. **114**, 1952–1959 (2016).
[35]Q. Wei, C. Zhao, M. Zhang, H. Yan, and B. Wei, "High-pressure phases and pressure-induced phase transition of MoN_6 and ReN_6," Phys. Lett. A **383**, 2429–2435 (2019).
[36]Y. Chen, X. Cai, H. Wang, H. Wang, and H. Wang, "Novel triadius-like N_4 specie of iron nitride compounds under high pressure," Sci. Rep. **8**, 10670 (2018).
[37]L. Wu, R. Tian, B. Wan, H. Liu, N. Gong, P. Chen, T. Shen, Y. Yao, H. Gou, and F. Gao, "Prediction of stable iron nitrides at ambient and high pressures with progressive formation of new polynitrogen species," Chem. Mater. **30**, 8476–8485 (2018).
[38]K. Niwa, K. Suzuki, S. Muto, K. Tatsumi, K. Soda, T. Kikegawa, and M. Hasegawa, "Discovery of the last remaining binary platinum-group pernitride RuN_2," Chem. - Eur. J. **20**, 13885–13888 (2014).
[39]A. F. Young, C. Sanloup, E. Gregoryanz, S. Scandolo, R. J. Hemley, and H. K. Mao, "Synthesis of novel transition metal nitrides IrN_2 and OsN_2," Phys. Rev. Lett. **96**, 155501 (2006).

[40]K. Niwa, D. Dzivenko, K. Suzuki, R. Riedel, I. Troyan, M. Eremets, and M. Hasegawa, "High pressure synthesis of marcasite-type rhodium pernitride," Inorg. Chem. **53**, 697–699 (2014).
[41]J. C. Crowhurst, A. F. Goncharov, B. Sadigh, C. L. Evans, P. G. Morrall, J. L. Ferreira, and A. J. Nelson, "Synthesis and characterization of the nitrides of platinum and iridium," Science **311**, 1275–1278 (2006).
[42]J. Li, L. Sun, X. Wang, H. Zhu, and M. Miao, "Simple route to metal *cyclo*-N_5^- salt: High-pressure synthesis of CuN_5," J. Phys. Chem. C **122**, 22339–22344 (2018).
[43]C. L. Schmidt, R. Dinnebier, U. Wedig, and M. Jansen, "Crystal structure and chemical bonding of the high-temperature phase of AgN_3," Inorg. Chem. **46**, 907–916 (2007).
[44]S. Krishnamurthy, M. Montalti, M. G. Wardle, M. J. Shaw, P. R. Briddon, K. Svensson, M. R. C. Hunt, and L. Šiller, "Nitrogen ion irradiation of Au(110): Photoemission spectroscopy and possible crystal structures of gold nitride," Phys. Rev. B **70**, 045414 (2004).
[45]J. H. Tian, T. Song, X. W. Sun, T. Wang, and G. Jiang, "Theoretical investigation on the high-pressure physical properties of ZnN in cubic zinc blende, rock salt, and cesium chloride structures," J. Phys. Chem. Solids **110**, 70–75 (2017).
[46]S. Guo, J. Lin, J. Li, Q. Wang, H. Wu, H. Zhu, and X. Wang, "High-pressure stable phases in mercury azide," Comput. Mater. Sci. **169**, 109147 (2019).
[47]B. A. Steele, E. Stavrou, J. C. Crowhurst, J. M. Zaug, V. B. Prakapenka, and I. I. Oleynik, "High-pressure synthesis of a pentazolate salt," Chem. Mater. **29**, 735–741 (2017).
[48]D. Laniel, G. Weck, G. Gaiffe, G. Garbarino, and P. Loubeyre, "High-pressure synthesized lithium pentazolate compound metastable under ambient conditions," J. Phys. Chem. Lett. **9**, 1600–1604 (2018).
[49]M. Bykov, E. Bykova, G. Aprilis, K. Glazyrin, E. Koemets, I. Chuvashova, I. Kupenko, C. McCammon, M. Mezouar, V. Prakapenka, H. P. Liermann, F. Tasnádi, A. V. Ponomareva, I. A. Abrikosov, N. Dubrovinskaia, and L. Dubrovinsky, "Fe-N system at high pressure reveals a compound featuring polymeric nitrogen chains," Nat. Commun. **9**, 2756 (2018).
[50]J. Binns, M.-E. Donnelly, M. Peña-Alvarez, M. Wang, E. Gregoryanz, A. Hermann, P. Dalladay-Simpson, and R. T. Howie, "Direct reaction between copper and nitrogen at high pressures and temperatures," J. Phys. Chem. Lett. **10**, 1109–1114 (2019).
[51]M. Bykov, T. Fedotenko, S. Chariton, D. Laniel, K. Glazyrin, M. Hanfland, J. S. Smith, V. B. Prakapenka, M. F. Mahmood, A. F. Goncharov, A. V. Ponomareva, F. Tasnádi, A. I. Abrikosov, T. Bin Masood, I. Hotz, A. N. Rudenko, M. I. Katsnelson, N. Dubrovinskaia, L. Dubrovinsky, and I. A. Abrikosov, "High-pressure synthesis of Dirac materials: Layered van der Waals bonded BeN_4 polymorph," Phys. Rev. Lett. **126**, 175501 (2021).
[52]S. Wei, D. Li, Z. Liu, W. Wang, F. Tian, K. Bao, D. Duan, B. Liu, and T. Cui, "A novel polymerization of nitrogen in beryllium tetranitride at high pressure," J. Phys. Chem. C **121**, 9766–9772 (2017).
[53]Y. Wang, J. Lv, L. Zhu, and Y. Ma, "CALYPSO: A method for crystal structure prediction," Comput. Phys. Commun. **183**, 2063–2070 (2012).
[54]Y. Wang, J. Lv, L. Zhu, and Y. Ma, "Crystal structure prediction via particle-swarm optimization," Phys. Rev. B **82**, 094116 (2010).
[55]J. P. Perdew, K. Burke, and M. Ernzerhof, "Generalized gradient approximation made simple," Phys. Rev. Lett. **77**, 3865–3868 (1996).
[56]J. D. Pack and H. J. Monkhorst, "'Special points for Brillouin-zone integrations'—A reply," Phys. Rev. B **16**, 1748–1749 (1977).
[57]G. Kresse and J. Furthmüller, "Efficient iterative schemes for *ab initio* total-energy calculations using a plane-wave basis set," Phys. Rev. B **54**, 11169–11186 (1996).
[58]P. E. Blöchl, "Projector augmented-wave method," Phys. Rev. B **50**, 17953–17979 (1994).
[59]K. Parlinski, Z. Q. Li, and Y. Kawazoe, "First-principles determination of the soft mode in cubic ZrO_2," Phys. Rev. Lett. **78**, 4063–4066 (1997).
[60]A. Togo, F. Oba, and I. Tanaka, "First-principles calculations of the ferroelastic transition between rutile-type and $CaCl_2$-type SiO_2 at high pressures," Phys. Rev. B **78**, 134106 (2008).
[61]S. Nosé, "A unified formulation of the constant temperature molecular dynamics methods," J. Chem. Phys. **81**, 511–519 (1984).
[62]W. G. Hoover, "Canonical dynamics: Equilibrium phase-space distributions," Phys. Rev. A **31**, 1695–1697 (1985).
[63]R. Hill, "Related content the elastic behaviour of a crystalline aggregate," Proc. Phys. Soc., London, Sect. A **65**, 349–354 (1952).
[64]Q. Zhang and Y. Chang, "Prediction of detonation pressure and velocity of explosives with micrometer aluminum powders," Cent. Eur. J. Energ. Mater. **9**, 77–86 (2012).
[65]M. J. Kamlet and J. E. Ablard, "Chemistry of detonations. II. Buffered equilibria," J. Chem. Phys. **48**, 36–42 (1968).
[66]S. Maintz, V. L. Deringer, A. L. Tchougréeff, and R. Dronskowski, "LOBSTER: A tool to extract chemical bonding from plane-wave based DFT," J. Comput. Chem. **37**, 1030–1035 (2016).
[67]W. Tang, E. Sanville, and G. Henkelman, "A grid-based Bader analysis algorithm without lattice bias," J. Phys.: Condens. Matter **21**, 084204 (2009).
[68]T. R. Galeev, B. D. Dunnington, J. R. Schmidt, and A. I. Boldyrev, "Solid state adaptive natural density partitioning: A tool for deciphering multi-center bonding in periodic systems," Phys. Chem. Chem. Phys. **15**, 5022 (2013).
[69]G. A. Olah, G. K. Surya Prakash, and G. Rasul, "N_6^{2+} and N_4^{2+} dications and their N_{12} and N_{10} azido derivatives: DFT/GIAO-MP2 theoretical studies," J. Am. Chem. Soc. **123**, 3308–3310 (2001).
[70]Q. S. Li and L. P. Cheng, "Aromaticity of square planar N_4^{2-} in the M_2N_4 (M = Li, Na, K, Rb, or Cs) species," J. Phys. Chem. A **107**, 2882–2889 (2003).
[71]L. P. Cheng and Q. S. Li, "N_4 ring as a square planar ligand in novel MN_4 species," J. Phys. Chem. A **109**, 3182–3186 (2005).
[72]G. van Zandwijk, R. A. J. Janssen, and H. M. Buck, "6π aromaticity in four-membered rings," J. Am. Chem. Soc. **112**, 4155–4164 (1990).
[73]L. P. Cheng and Q. S. Li, "Theoretical study of nitrogen-rich BeN_4 compounds," J. Phys. Chem. A **108**, 665–670 (2004).
[74]Z. J. Wu, E. J. Zhao, H. P. Xiang, X. F. Hao, X. J. Liu, and J. Meng, "Crystal structures and elastic properties of superhard IrN_2 and IrN_3 from first principles," Phys. Rev. B **76**, 054115 (2007).
[75]M. Moreno Armenta, A. Reyes-Serrato, and M. Avalos Borja, "*Ab initio* determination of the electronic structure of beryllium-, aluminum-, and magnesium-nitrides: A comparative study," Phys. Rev. B **62**, 4890–4898 (2000).
[76]C. J. Pickard and R. J. Needs, "High-pressure phases of nitrogen," Phys. Rev. Lett. **102**, 125702 (2009).
[77]M. J. Kamlet and C. Dickinson, "Chemistry of detonations. III. Evaluation of the simplified calculational method for Chapman-Jouguet detonation pressures on the basis of available experimental information," J. Chem. Phys. **48**, 43 (1968).
[78]J. Zhang, A. R. Oganov, X. Li, and H. Niu, "Pressure-stabilized hafnium nitrides and their properties," Phys. Rev. B **95**, 020103(R) (2017).
[79]J. P. Agrawal, *High Energy Materials: Propellants, Explosives and Pyritechnics* (J. Stierstorfer and T. M. Klapötke, 2010).
[80]G. T. Furukawa and M. L. Reilly, "Heat capacity and thermodynamic properties of α-beryllium nitride, Be_3N_2, from 20 to 315 K," J. Res. Natl. Bur. Stand., Sect. A **74A**, 617–629 (1970).
[81]T. B. Douglas and W. H. Payne, "Measured enthalpy and derived thermodynamic properties of alpha beryllium nitride, Be_3N_2, from 273 to 1200 K," J. Res. Natl. Bur. Stand., Sect. A **73A**, 471–477 (1969).
[82]D. Hall, G. E. Gurr, and G. A. Jeffrey, "Zur kenntnis des systems Be_3N-Si_3N_4. V. A refinement of the crystal structure of β-beryllium nitride," Z. Anorg. Allg. Chem. **369**, 108–112 (1969).
[83]D. Laniel, B. Winkler, T. Fedotenko, A. Pakhomova, S. Chariton, V. Milman, V. Prakapenka, L. Dubrovinsky, and N. Dubrovinskaia, "High-pressure polymeric nitrogen allotrope with the black phosphorus structure," Phys. Rev. Lett. **124**, 216001 (2020).
[84]C. Lin, X. Liu, X. Yong, J. S. Tse, J. S. Smith, N. J. English, B. Wang, M. Li, W. Yang, and H.-K. Mao, "Temperature-dependent kinetic pathways featuring distinctive thermal-activation mechanisms in structural evolution of ice VII," Proc. Natl. Acad. Sci. U. S. A. **117**, 15437–15442 (2020).
[85]C. Lin, X. Liu, D. Yang, X. Li, J. S. Smith, B. Wang, H. Dong, S. Li, W. Yang, and J. S. Tse, "Temperature- and rate-dependent pathways in formation of metastable silicon phases under rapid decompression," Phys. Rev. Lett. **125**, 155702 (2020).